


Differential effects of climate change on average and peak demand for heating and cooling across the contiguous USA

Yash Amonkar ^{1,2}, James Doss-Gollin ³, David J. Farnham⁴, Vijay Modi ⁵ & Upmanu Lall ^{1,2}

While most electricity systems are designed to handle peak demand during summer months, long-term energy pathways consistent with deep decarbonization generally electrify building heating, thus increasing electricity demand during winter. A key question is how climate variability and change will affect peak heating and cooling demand in an electrified future. We conduct a spatially explicit analysis of trends in temperature-based proxies of electricity demand over the past 70 years. Average annual demand for heating (cooling) decreases (increases) over most of the contiguous US. However, while climate change drives robust increases in peak cooling demand, trends in peak heating demand are generally smaller and less robust. Because the distribution of temperature exhibits a long left tail, severe cold snaps dominate the extremes of thermal demand. As building heating electrifies, system operators must account for these events to ensure reliability.

¹Columbia Water Center, Columbia University, New York, NY, USA. ²Department of Earth and Environmental Engineering, Columbia University, New York, NY, USA. ³Department of Civil and Environmental Engineering, Rice University, Houston, TX, USA. ⁴ClimateAI, San Francisco, CA, USA. ⁵Department of Mechanical Engineering, Columbia University, New York, NY, USA. email: yva2000@columbia.edu

Extreme weather events pose an operational risk to infrastructure systems and the humans who depend on them and are a major cause of power outages and energy price spikes across the United States^{1–3}. Hot (cold) temperatures create a demand for cooling (heating), which in turn drive demand for energy. For example, Winter Storm Uri, which caused cascading failures through interconnected and interdependent infrastructure systems as well as loss of human life in Texas in 2021, was caused not only by supply-side failures of the energy system⁴ but also by unanticipated surges in demand for heating². Similarly in August 2020, an extreme heat wave in California caused surging demand for cooling, leading the grid operator to institute rolling blackouts⁵.

This problem is not limited to the electricity sector. Severe winter weather in New England can lead to scarcity-driven spikes in wholesale prices of electricity and natural gas³. At present, peak electric load events across the contiguous United States (CONUS) occur during the summer months and when high temperatures lead to demand for electricity to power air-conditioning. A large fraction of energy demand for heating during the winter is met by gas or oil furnaces⁶. However, modeled pathways to deep decarbonization typically require electrification of sectors including building heating⁷, which may lead to peak demands for electricity during winter cold spells⁸. Because winter temperatures are typically farther from a thermal comfort level than summer temperatures, electrification of space-heating will change the seasonality of electricity demand, with large portions of the United States projected to become winter peaking systems^{8,9}. Thus, a key question is how climate variability and change will affect peak demands for heating and cooling in an electrified future.

Theory and climate models offer important insights on this question. In general, anthropogenic climate change drives robust increases in surface temperatures globally¹⁰. If this were to lead to a shift in the distribution of temperatures without a change in the variability, then demand for heating would decrease and demand for cooling would increase. However, warming trends are accompanied by changes in the severity and duration of extreme weather events such as heat waves¹¹, which are particularly important to understand in order to maintain a reliable power grid and provide space cooling to alleviate dangerous level of heat within urban settings¹². Overall, shifts in the average temperature are better understood than shifts in the extremes, particularly cold extremes. While broad scientific consensus points to increasing frequency and magnitude of heat waves¹³, long-term changes in frequency of mid-latitude winter extreme temperatures or cold snaps are uncertain potentially driven by Arctic Amplification and remain an active area of research^{14,15}.

In this paper, we present a retrospective analysis of trends in heating and cooling demand using temperature-based proxies of energy demand for the last 72 years (1950–2021) over the CONUS using climate reanalysis data¹⁶. Throughout this paper, the cooling or heating demand refers to the inferred cooling or heating demand computed solely using temperature-based proxies. We have not considered the non-linearities in peak demand that occur, particularly at extreme temperatures due to humidity (cooling), installed heating system capacity and technology, building occupancy, demographics, housing stock and price elasticity. The lack of place-specific data for these considerations and the dependence on legacy building stock envelope would preclude nation-wide comparisons if one attempts to account for these non-linearities. We quantify both changes to annual average energy demand and to annual maximum (peak) energy demands, which are key design parameters for energy and electricity systems^{17,18}. Moreover, peak load supply is generally more expensive compared to ordinary supply plants and

contributes disproportionately to consumer costs. We focus on understanding historical trends and their system reliability implications for near-term operations and investment, given that in the long term deeply uncertain technological and socio-economic factors will drive system performance¹⁹. The primary focus of the study, to examine the changing capacity requirements and load factors, within the context of all heating and cooling demand met increasingly by electricity, has clear implications for future grid cost structures. We identify a north-south divide in the emergent patterns of the heating, cooling, and total thermal demand trends, especially for the ratio of average to peak demands and the relative importance of the peak cooling and peak heating demand. To aggregate findings to decision-relevant scales, we estimate trends for major electric grid systems and present findings for Florida and the Midcontinent Independent System Operator (MISO), which serve as the archetypes of the grid in the north and south.

Results and discussion

Trends in annual mean inferred thermal demand. Mean heating and cooling demand contribute to the total demand for energy and have direct implications for carbon emissions and energy economics. A first question is how the average annual demand for heating and cooling has changed over the past 70 years. To answer this question, we consider the average annual demand for cooling and heating inferred from hourly temperature data from the ERA-5 reanalysis dataset¹⁶. Specifically, we define the inferred demand for heating and cooling following Doss-Gollin et al.², at each grid cell and for each hour, as the difference between the hourly temperature and a threshold temperature of 65 F; see Methods for additional details. These can be interpreted as the number of degrees a building must be cooled or heated to reach a thermal comfort level. We also define the total thermal demand as the sum of the cooling and heating demand. Mean inferred cooling, heating and total thermal demand across the CONUS is displayed in Fig. S1.

Figure 1 shows robust increases in annual demand for cooling and robust decreases in demand for heating across the CONUS. This is consistent with first-order expectations from climate change, which is expected to increase the temperature and length of summers and to shorten the length and severity of winters²⁰. The dark red regions, especially in central Colorado, show the largest increases in demand for cooling, with the trend being >1%/year, and the dark blue regions, especially in the southern Florida, show the largest decreases in demand for heating, with the trend being below –1%/year. This is also consistent with expectations about regional climate change in southern Florida²¹ and in Colorado with higher elevations generally recording higher warming rates²² and could be driven by changes in the snow telemetry stations²³. Similar trends in annual mean inferred demand across CONUS in terms of raw magnitude are shown in Fig. S2.

These competing shifts lead to different trends in total thermal demand by region. Across most of CONUS, total thermal demand shows robust negative trends because winters are longer and farther from a thermal comfort level than summers. However, in southern states where summers are particularly long and hot, the increased demand for cooling outweighs the decreased demand for heating; these trends are significant in some parts of Florida, Arizona, Texas, and Southern California. Field significance tests (see Methods) reject the hypothesis of no trend for all three demand types.

While analysis at the scale of reanalysis grid cells is useful for understanding the spatial patterns of trends, it is not directly relevant to the operation of the electric grid. Electric Grids,

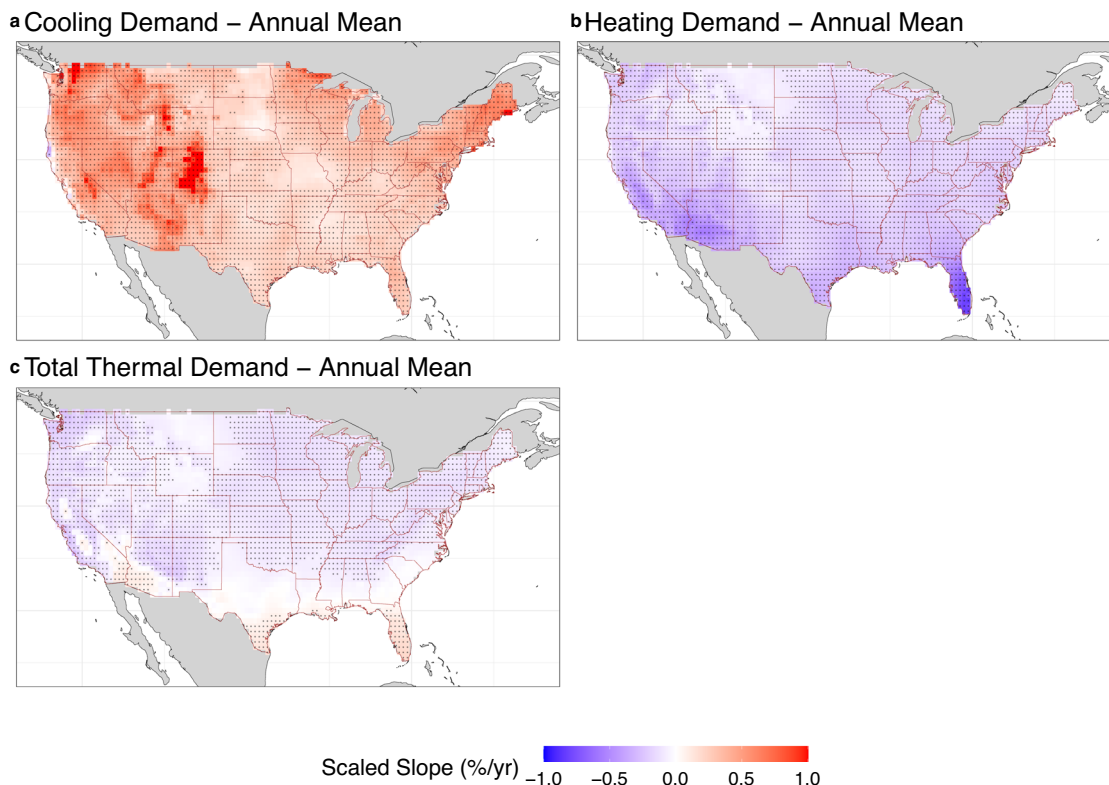


Fig. 1 Demand for cooling (heating) is increasing (decreasing) across the contiguous United States (CONUS), with net decreases in all but the hottest climates. Trends (see Methods for details) in annual mean demand for (a) cooling, (b) heating, and (c) total thermal demand across the CONUS at each grid cell ($0.5^\circ \times 0.5^\circ$ lat-lon) from ERA5¹⁶. The shaded colors denote the estimated trend per year (%/year). The dotted regions are locations where the trend in the mean inferred demand is statistically significant at the 5% level.

Independent System Operators, and Regional Transmission Operators are socio-political entities over which grid planning and operations are coordinated. Such entities have boundaries of operation and serve dedicated population centers and regions. As such, ensuring adequate supply and reliability of electricity is a key concern for these entities. Moreover, electric grids are designed for the peak load and increasing electric generation capacity is capital intensive and requires analysis of forecasts and trends in projected demand¹⁷. To answer this question, we aggregate the thermal trends over space, weighing each grid cell by its 2020 population²⁴.

Figure 2 shows the aggregated trends in the total thermal demand for the Florida Electric Grid and the Midcontinent Independent Systems Operator (MISO), which are representative of the hot and cold regions of the CONUS, respectively. The Florida grid (Fig. 2a) covers most of the state of Florida, with the exception of the panhandle and is the southernmost sub-grid within the CONUS. Like other southern regions, average inferred cooling demand is greater than the average inferred heating demand, and so the net trend is towards increasing total thermal demand (Fig. 2c). Florida is the only grid entity within the CONUS (see Methods for a list of all entities examined) where the total thermal load has a statistically significant increasing trend.

An opposite trend is apparent for the region served by MISO (Fig. 2b). Because of its northern location, MISO has an inferred heating demand much larger than the inferred cooling demand (Fig. 2d). Consequently, the increasing background temperature leads the decreasing heating demand to dominate the total thermal demand, resulting in a net decrease in total thermal demand. This trend is representative for other grid entities serving northern regions (Fig. S3–S5). This indicates that a

scenario with total electrification of space heating would see decreasing demand on average across the Northern CONUS.

Trends in annual peak inferred thermal demand. Although the annual mean thermal demand is a useful metric for understanding the long-term trends in thermal demand, an equally important metric is the peak thermal demand. Designing a system for peak demand is important for ensuring reliability of the electrical¹⁷ and other energy systems³. Peak electrical demands are already projected to increase as other sectors of the economy (e.g., transportation) electrify²⁵. To analyze the presence of temperature-driven trends in the inferred peak demand we examine the time series of the annual maximum (instead of annual mean considered in the previous section) 72-h inferred thermal demand from the same datasets. The effect of extreme temperature events on energy demand is a function of the event's length and intensity with short term spikes interrupting plant operations and spiking prices while long duration events also causing breakdown of critical infrastructure services. Similar analysis was also carried out for peak inferred demand events for durations ranging from 6 h to 336 h (14 days).

Consistent with a background increase in temperature, increases (decreases) in peak demand for cooling (heating) are observed across large swaths of CONUS (Fig. 3a, b). Across large swaths of the CONUS, the peak inferred cooling demand intensity (duration 72 h) has increased, whereas the peak inferred heating demand intensity has decreased. The peak total thermal load also shows decreasing trends throughout the CONUS, except for the southernmost regions (Fig. 3c). Furthermore, we find no systematic shift or change in the seasonality and day-of-year occurrence of peak inferred heating and cooling demand events.

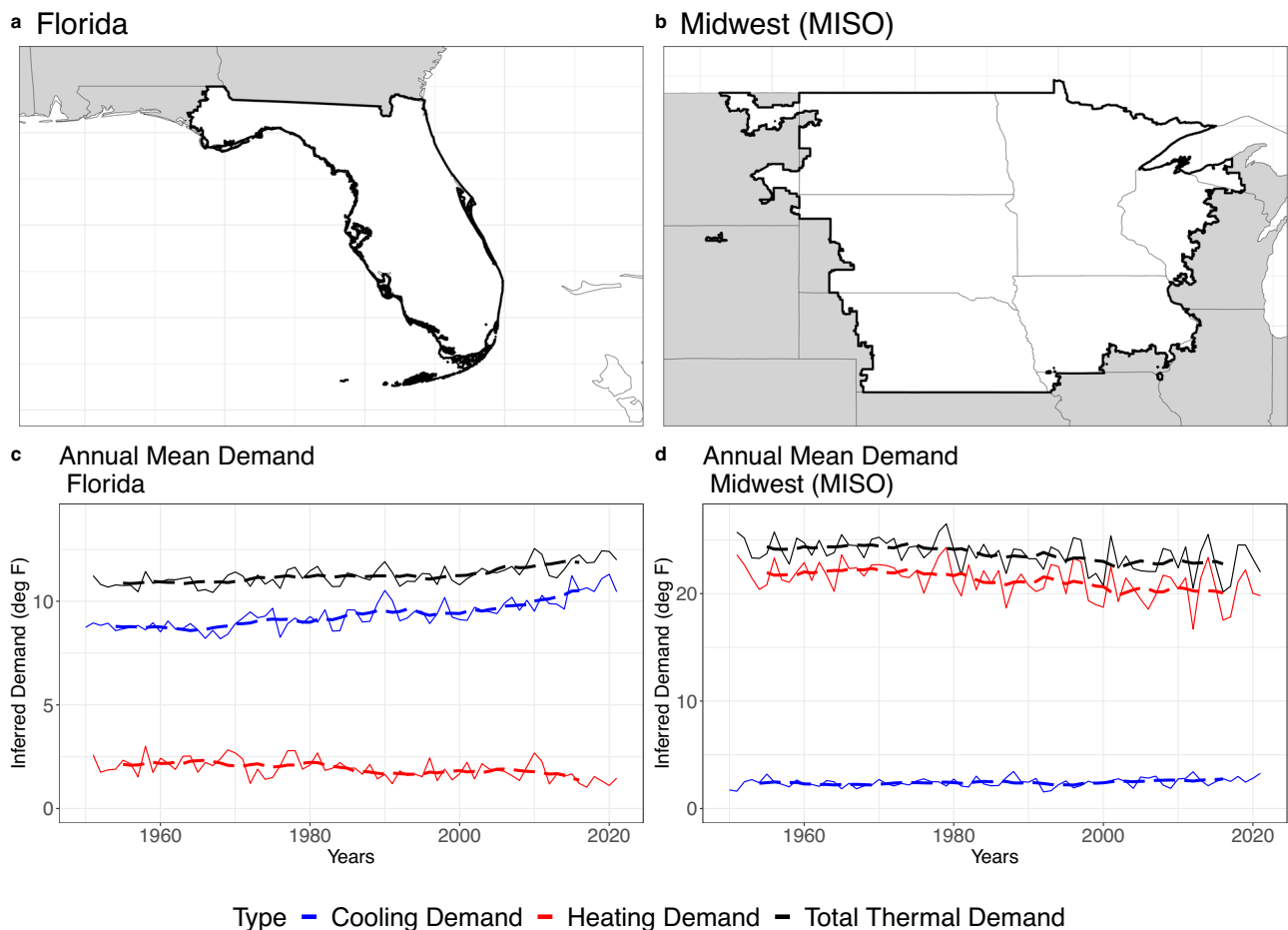


Fig. 2 While demand for heating (cooling) is decreasing (increasing) across the contiguous United States (CONUS), the net effect is a decrease in total thermal demand in cold regions and a net increase in total thermal demand in hot regions. Two archetypes of grid operators serving hot (a) Florida and cold (b) MISO regions are shown. c Annual mean inferred demand in terms of degrees Fahrenheit for Florida. d Annual mean inferred demand in terms of degrees Fahrenheit for MISO. Red lines show decreasing demand for heating, blue lines show increasing demand for cooling, and black lines show increasing (decreasing) total thermal demand for Florida (MISO). The dashed lines denote the 10-year moving average.

Field significance tests were also run and the hypothesis of no trend was rejected for all three demand types. Similar trends in intensity of peak inferred demand across CONUS in terms of raw magnitude are shown in Fig. S6.

The peak inferred cooling demand intensity for events with a duration of 72 h (Fig. 3a) shows increasing trends across most of the CONUS. The median trend is 0.16%/yr, whereas the range extends from $-0.25\%/year$ to $1.77\%/year$. The estimated slope of the trend is largest in central Colorado, with an annual increase $>1\%/year$. Almost all of the western United States, New England, New York, Florida, Louisiana, Pennsylvania and large portions of Texas, Virginia, and North Carolina have increasing cooling demand intensity trends that are statistically significant. This is in contrast to interior regions of the Midwest and the Plains, which exhibit smaller trends, and the Dakotas, which even exhibit a small decreasing trend in the peak cooling demand. Similar trends, including the large increases within Colorado and decreases within the Dakotas, are seen in peak events when other event durations are considered (Fig. S7).

Almost the entire CONUS has had decreasing trends in the peak inferred heating demand intensity for events with a duration of 72 h (Fig. 3b). The median trend is $-0.1\%/year$, with the range being $(-0.41, 0.03) \%/yr$. Unlike the peak cooling demand intensity, there are no areas with large increases and the trends are significant mostly in Southern California and the southwest

and southeast portions of the CONUS, which are regions where the heating demand during the winter is low and does not dominate grid operations. The nature of the trends in peak heating event intensity is fairly constant across multiple durations (Fig. S8).

Trends in peak inferred thermal load intensity for events for a 72 h duration (Fig. 3c) have a median and range of $-0.1 \%/year$ and $(-0.37, 0.20) \%/year$, respectively. The statistically significant trends are concentrated in the southern parts of the Western United States, from Appalachia to Florida and in the upper Northeast of the country. Almost all of the CONUS shows an overall decrease in the peak thermal load intensity driven by the decrease in the peak heating demand intensity (Fig. 3b), which is typically larger than the peak cooling demand intensity. Exceptions are the southernmost parts of Florida, Texas, Arizona, and California, where there is an increase driven by the peak cooling demand intensity that exceeds the peak heating demand intensity. Trends for other event durations have similar spatial patterns (Fig. S9).

The secular trends that were present in the mean heating, cooling, and total thermal demand (Fig. 2) are less prominent in the peak events for both Florida and MISO (Fig. 4). Instead, the peak heating demand is marked by substantial inter-annual and decadal variability (Fig. 4). Florida has an increasing peak cooling demand trend and a recent decline in the peak heating demand

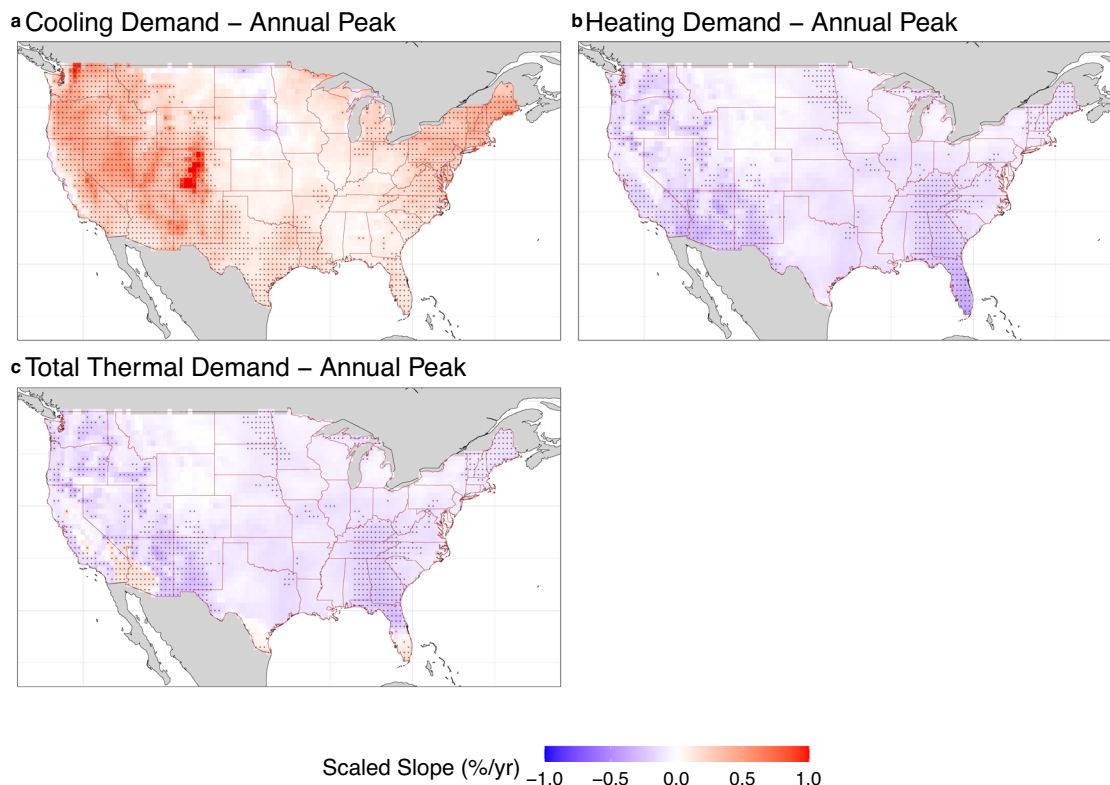


Fig. 3 Trends in the intensity of peak inferred cooling, heating, and total thermal demand across the CONUS are more variable than the trends in the mean demands but are most coherent for cooling demand in the Western and Northeastern portions of the CONUS, where cooling demands have been increasing. Trends in the intensity of peak inferred demand events of duration 72 h for (a) cooling demand, (b) heating demand, and (c) total thermal demand at the reanalysis grid-cell level ($0.5^\circ \times 0.5^\circ$ lat-lon) across the CONUS. The shaded colors denote the estimated trend per year (%/yr). The dotted regions are locations where the trend in demand is statistically significant at the 5% level. Peak events correspond to the annual maximum events (see Methods for further details).

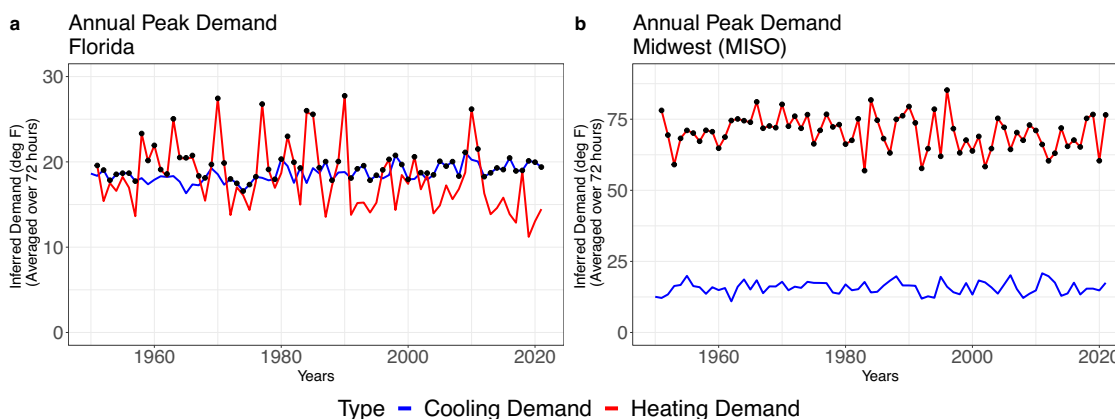


Fig. 4 The magnitude of inter-annual variability in the intensity of peak heating events is much larger than that of peak cooling events, as shown for both Florida and the Midwest (MISO). Peak Inferred Demand Intensity for events of duration 72 h in population adjusted degrees Fahrenheit averaged over 72 h for (a) Florida, and (b) MISO. The red and blue colors correspond to heating and cooling demand, respectively. The black dots correspond to peak events for the total thermal load.

intensity. Such trends are not evident for MISO. Similar plots of the peak inferred demand intensity for other grid sub-regions are attached in the supplement (Fig. S10–S12).

The peak event intensity for total thermal load for Florida (Fig. 4a), is typically associated with the peak cooling demand, but dramatically higher peak heating demands occur in several years corresponding to cold outbreaks. The peak cooling demand events dominate post 2010. Thus, for grid operators in the Southern United States, a challenge is the variability in the peak heating

demand, which far exceeds the variability in the peak cooling demand. For MISO (Fig. 4b), the peak total thermal demand events are exclusively the peak heating demands, exhibiting increasing inter-annual variability post 1980. Consequently, a seasonal prediction for the winter to anticipate either a high or a low heating demand peak is crucial for timing system maintenance and upgrades and allocating adequate capacity. For example, the planned outages for plant maintenance coincided during the Texas freeze of Feb 2021^{2,4}, in anticipation of a future summer peak.

Trends in thermal load factors. An additional measure of grid operation viability is the load factor²⁶, which is a measure of the efficiency of electricity usage. The load factor is defined as the ratio of average load to peak load over a specific time interval. It measures the average utilization of the installed capacity of electric infrastructure systems. While the overall grid economics are determined by numerous factors, including governmental policies, the peak loads and load factors are indicators of the overall supply-side economics of the grid.

The utilization of installed system capacity is a key criterion in energy economics and infrastructure management²⁷. Infrastructure utilization is often measured by a load factor defined as the annual mean demand divided by the peak demand for the same year. In this section, we look at only how climate affects utilization rates. Demand fluctuations for other reasons for example, population and efficiency of technology, are amplified by thermal load considerations. The installed capacity should be determined by the expected peak demand. In the current context, we consider the peak thermal demand as the design criteria, assuming that it is the dominant additive determinant of the peak load on the system, and consider the utilization factor through the ratio of the mean thermal load to the peak thermal load.

Large portions of the southern United States show an increasing trend in thermal load factors, though trends are statistically significant only in the southernmost regions. The trends in the infrastructure utilization rates (load factors) for thermal demand are shown in Fig. 5. The median and range of the trends are 0.01 %/yr and (−0.17, 0.42) %/yr, respectively. For example, within the Florida grid sub-region (Fig. 6a), thermal load factors show an increasing trend with large decadal variability, mirroring our earlier observation of the peak heating trend. A silver lining is that while the peak thermal load in Florida (Fig. 4a) is increasing, the mean thermal load is increasing faster, translating into higher load factors or greater utilization of the needed capacity. A much milder trend (decreasing mainly in the 1950s) is evident for MISO (Fig. 6b). There is high inter-annual variability in the load factor for both MISO and Florida, largely due to dramatic year-to-year changes in the peak heating load, re-emphasizing the importance of accurate seasonal forecasts for the

peak heating load or winter cold outbreaks. Similar trends in thermal load factors across CONUS in terms of raw magnitude are shown in Fig. S13.

The northern parts of the CONUS and parts of the Western mountain regions have decreasing load factor trends (significant in parts of California, and the Great Lakes region) (Fig. 5). The mean thermal load is decreasing faster than the peak in these areas. Few areas, including parts of Southern California and Arizona, are driven by different dynamics, where the decreasing load factors are driven by slower increases in the mean thermal demand than the peak. These trends are similar for other event durations (Fig. S14). Further, plots of the load factors for other grid sub-regions are attached in the supplement (Figs. S15–S17).

Similarly, these predominant trends in Florida and MISO are also visualized in load duration curves²⁸ that represent the relative frequency of demand exceedance (Fig. S18). The load duration curves for other grid sub-regions are attached in the supplement (Figs. S19–S21). Overall, the ongoing process of electrification of space-heating is poised to increase the actual electric peak load across large parts of the country⁸. Once completed, however, the infrastructure built to meet the peak load may see lower utilization rates in the northern parts of the United States driven by decreases in the mean heating demand (Fig. 1), which are larger than the decreases in peak demand (Fig. 3). Lower infrastructure utilization rates are associated with higher average operating costs that are then passed on to consumers.

Conclusions

As expected under a global warming regime, there have been significant changes in the thermal loads experienced by electric grid operators across the CONUS. Overall, the average winter heating demand is decreasing, whereas the average summer cooling demand is increasing. The dynamics are less consistent in the case of peak load events, where the peak heating load is relatively unchanged across large swaths of the CONUS while the peak cooling load is increasing in the population dense regions.

There are divergent trends in the hypothetical capacity utilization over the historical record that impact regional energy economics. The average heating demand is decreasing faster than the peak heating demand, leading to decreasing load factors in the northern regions of the CONUS, where the heating load dominates the grid. In the southernmost regions of the CONUS, where cooling loads dominate, the average cooling demand is increasing faster than the peak cooling demand, leading to increasing load factors. If these divergent trends in capacity utilization are manifest, due to widespread electrification of heating, and continue into the future, they will effectively result in progressively increasing costs needed to maintain reliable power systems in northern regions of the CONUS and decreasing costs needed to maintain reliable power systems in southernmost areas of the CONUS. In fact, this analysis is a precursor to evaluating results from climate model simulations of future climate conditions. The results presented in this paper apply to temperature induced changes (which in turn are linked to climatic changes) in cooling or heating requirements. They do not account for dependence on humidity, housing stock, occupancy, or state of deployment of specific heating and cooling technologies. Extrapolation of these results outside the CONUS regions, in particular cities in the global South, is complicated by the rapid adoption of air-conditioning and a corresponding increase in electric demand, in contrast to the CONUS, where the air-conditioning levels have stabilized²⁹.

Thermal Load Factor

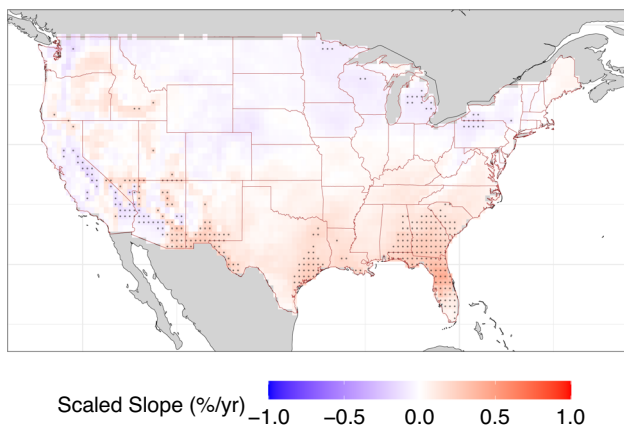


Fig. 5 Trends in the thermal load factors across the CONUS are heterogeneous, with a spatially coherent pattern of positive trends in the Southeastern US. Trends in load factors for total thermal demand at the grid-cell level ($0.5^\circ \times 0.5^\circ$ lat-lon) across the CONUS. The peak event demand intensity is computed for events with a duration of 72 h. The shaded colors denote the estimated trend per year (%/year). The dotted regions are locations where the trend in the load factors is statistically significant at the 5% level.

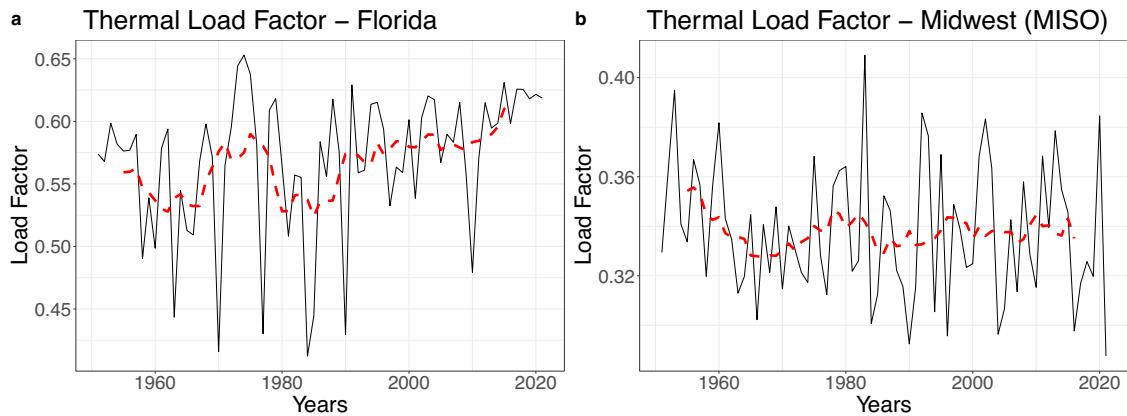


Fig. 6 Trends in the annual thermal load factors are contrasting for Florida (increasing) and Midwest (MISO; slightly decreasing), though both regions exhibit substantial inter-annual and inter-decadal variability. Annual Load factors for total thermal load for (a) Florida, (b) MISO. The load factors are defined as the annual mean load divided by the annual peak load. Peak demand load is computed for events of a duration of 72 h. The dashed red line denotes the 10-year moving average.

Lastly, our results show that peak heating demand during winter is characterized by very high inter-annual variability. This variability is difficult to manage without procuring massive reserve capacity during winter and/or improving our ability to predict such winter peak events with sufficient lead times to adjust normal system operations, such as by postponing regular seasonal maintenance. We recently witnessed some of the significant electric grid problems that can occur due to poor anticipation of a severe cold outbreak in Texas in 2021 during winter storm Uri².

Methods

Temperature. The 2-meter surface temperature data are taken from ERA-5 reanalysis data product¹⁶. The spatial grid size of the data is set at 0.5° lat \times 0.5° lon and contains 3267 grid points within the contiguous United States (Fig. S22A). The data are at an hourly time-step and span 72 years (1950–2021).

Population. The population data are taken from the Gridded Population of the World, Version 4 (GPWv4)²⁴. The population for the year 2020 is used in this study. The data files were produced as global rasters at 30 arc-second (1 km at the equator) resolution but aggregated to the spatial resolution of the reanalysis dataset.

Electric grid sub-regions. The CONUS is divided into three major grids—Western Interconnection, Eastern Interconnection, and Electric Reliability Council of Texas. These three interconnections are further divided into Regional Transmission Organizations, Independent System Operators, and additional sub-regions. We use the Environmental Protection Agency’s (EPA) Emissions & Generation Resource Integrated Database (eGRID) maps for the shape-files of the various grid sub-regions³⁰. The eGRID sub-regions are regional entities of EPA’s Clean Air Markets Division and roughly correspond to the grid sub-regions. We make the following changes in the shape-files to have the eGRID sub-regions better reflect the grid subregions. The eGRID sub-regions of New York City, Long Island, and New York State are merged to better reflect the New York Independent System Operator (NYISO), which covers the entire state of New York. The spatial extent of the grid sub-regions is shown in Fig. S22B. The list of the grid entities analyzed in this study are (A) Arizona/New Mexico, (B) CAISO, (C) ERCOT, (D) Florida,

(E) Wisconsin (Rural), (F) Midwest (MISO), (G) ISO New England, (H) Northwest, (I) NYISO, (J) PJM (West), (K) Michigan, (L) PJM (East), (M) Colorado, (N) Kansas, (O) Oklahoma, (P) Arkansas/Louisiana, (Q) Missouri, (R) Southeast, (S) Tennessee Valley, (T) Carolinas (Fig. S22B).

Inferred heating, cooling and total thermal demand at the local level. The local inferred demand is computed for each grid-cell where the ERA-5 temperature data are available. The residential heating and cooling demand are functions of the temperature deviation from a temperature most suited for human comfort⁸. The total thermal demand is defined as the sum of both the heating and cooling demand (total temperature dependent inferred demand).

Using 65 F (18.33 °C, 291.5 K) as the ambient temperature threshold, the deviation of observed temperature from this threshold is taken as the proxy inferred heating and cooling demand. Our overall conclusions are not sensitive to the ambient temperature threshold. Different thresholds (e.g., 68 F) also lead to similar macro level trends. The ERA-5 data are available at an hourly resolution and the inferred heating and cooling demand was computed as

$$HD_{i,t} = \max(65 - T_{i,t}, 0) \quad (1)$$

$$CD_{i,t} = \max(T_{i,t} - 65, 0) \quad (2)$$

$$TTD_{i,t} = |T_{i,t} - 65| \quad (3)$$

where, $HD_{i,t}$, $CD_{i,t}$, $TTD_{i,t}$ and $T_{i,t}$ are the inferred heating demand, inferred cooling demand, inferred total thermal demand, and observed temperature at hour t and location i .

Population distribution weighted inferred demand at the regional level. All the ERA-5 temperature locations (grid-cells) within the electric grid sub-region of interest are identified and the inferred thermal demand is computed for each grid-cell using the method described above. The grid-cell level inferred demand is then multiplied by the regional population fraction associated with that location (grid-cell) and summed across all locations (grid-cells) within the electric grid sub-region of interest. The population weighted inferred heating, cooling, and total thermal

demand are defined as,

$$HD_t = \sum_{i=1}^N \max(65 - T_{i,t}, 0) \times f_i \quad (4)$$

$$CD_t = \sum_{i=1}^N \max(T_{i,t} - 65, 0) \times f_i \quad (5)$$

$$TTD_t = \sum_{i=1}^N |T_{i,t} - 65| \times f_i \quad (6)$$

Where, HD_t , CD_t , and TTD_t are the population adjusted inferred heating, cooling and total thermal demand for hour t . $T_{i,t}$ is the observed temperature for location i at hour t . N is the total number of ERA-5 temperature grid-cells within the grid sub-region of interest. f_i is the population fraction associated with the grid-cell i . The 2020 population was used to assess the population fractions f_i . Thus, the trends computed are sensitive to temperature only, and not to population changing over time.

Peak inferred demand. We use the annual maxima of the thermal load over a particular duration (e.g., a moving window of 72 h) as the criteria to define peak events³¹. This relates directly to the generation capacity needed for grid operations as an addition to other loads. The annual maximum peak intensity of heating, cooling or total thermal demand for an event of duration 72 h is computed as

$$I_y = \max_t \left(\sum_{t=m}^{m+71} ID_{t|y} \right) \quad 1 < m < (n - 72), y = 1 \dots k \quad (7)$$

where, I_y is the peak demand intensity for year y for events of duration 72 h, ID_t is the inferred demand for hour t . n is the total number of hours t in year y , and k is the total number of years.

The annual cycle for identifying peak inferred cooling demand events is set as January–December, whereas the annual cycle for identifying peak inferred heating and total thermal demand events is set as September–August. This ensures seasonal continuity since the peak inferred heating demand events occur most frequently during the boreal winter (December–January–February). A consequence of this transformation is that peak inferred cooling demand data extends from 1950–2021 (72 year), whereas the peak inferred heating and total thermal demand data spans only 1951–2021 (71 years). Options for computing the inferred heating and cooling demand that incorporate non-linearities in response to the peak demand in addition to the threshold-based non-linearities exist in the literature^{32–34}. Overall such methods generalize poorly spatially across the CONUS due to multiple factors, and we use the metric described above to focus on temperature driving changes.

Trend analysis for direction. The Mann–Kendall (MK) trend test is used to check for the presence of a monotonic trend in the time series data and is a non-parametric rank based test making it applicable to any data irrespective of the underlying generative probability distribution³⁵. The two-sided MK test is used to check for the presence of either a monotonic increasing or decreasing trend in the data. The MK test statistic (Z_s) for a time series x_1, x_2, \dots, x_n is computed as:-

$$S = \sum_{i=1}^{n-1} \sum_{j=i+1}^n \text{sgn}(x_j - x_i) \quad (8)$$

Where, sgn is the sign operator taking values $-1, 0, 1$ for the

negative, zero and positive values respectively.

$$Z_s = \begin{cases} \frac{S-1}{\sigma} & \text{if } S > 0 \\ 0 & \text{if } S = 0 \\ \frac{S+1}{\sigma} & \text{if } S < 0 \end{cases} \quad (9)$$

The null hypothesis of this test is rejected at significance level α if $|Z_s| < Z_{crit}$ where Z_{crit} is the value of the standard normal distribution with a probability of exceedance of $\alpha/2$. The significance level selected for this study is 5%. Refer³⁵ for additional details on computation of σ_s and effect of the sample size n .

Trend analysis for slope. Thiel-Sen slope (b_s), a rank based test statistic, is computed as a robust estimate of the monotonic trend. The estimate, a median of the pairwise slopes between elements of the series, is based on a non-parametric test and can be applied to all distributions. The validity of this test does not depend on the normality of the residuals and is not strongly affected by outliers, unlike ordinary least square regression³⁵.

The estimate is computed using each pair of observations in a pairwise manner, resulting in $n \times (n - 1)/2$ individual computations. For each data pair the slope between the two points is computed. The median of all such values is the required slope. The significance test for the slope is identical to the procedure above.

$$b_s = \text{median} \left(\frac{y_j - y_i}{x_j - x_i} \right) \quad (10)$$

The Mann–Kendall trend test and Thiel-Sen’s slope estimation were conducted using the trend package³⁶.

Field significance test. The field significance test is used to check whether the total number of tests that show a significant result could have happened by chance, given that a large number of tests were conducted. The null hypothesis of this test is that the fraction of grid cells exhibiting a monotonic linear trend at $\alpha\%$ level of significance can be attributed to random chance and spatial correlation between the grid cells^{37,38}. The test is conducted using a bootstrap that resamples the entire field by time, thus addressing the potential spatial correlation in the data.

For each bootstrap sample, the significance test described earlier is run at all the grid points. The total number of grid points that turn up significant are noted. This procedure is repeated for 1000 bootstrap samples. The $(1 - \alpha)^{\text{th}}$ percentile of the number of grid points significant for the 1000 bootstrapped samples is compared against the data. If the number of significant grid-points in the data is greater than the $(1 - \alpha)^{\text{th}}$ percentile from the bootstrapped copies, the null hypothesis of the field significance test at the $\alpha\%$ level of significance is rejected³⁸.

Data availability

The ERA-5 temperature data, population data, and grid sub-region shapefiles can be accessed publicly with the details of the data sources provided in the Methods section. All code and data used in this study is made publicly available at <https://zenodo.org/record/8395835>.

Code availability

The code used in this study is made publicly available in a GitHub repository and can be accessed from <https://github.com/yashamonkar/CONUS-Inferred-Heating-Cooling>.

Received: 19 March 2023; Accepted: 10 October 2023;

Published online: 01 November 2023

References

- Smith, A. U. S. *Billion-dollar Weather and Climate Disasters*. <https://www.ncei.noaa.gov/access/metadata/landing-page/bin/iso?id=gov.noaa.nodc:0209268> (2022).
- Doss-Gollin, J., Farnham, D. J., Lall, U. & Modi, V. How unprecedented was the February 2021 Texas cold snap? *Environ. Res. Lett.* **16**, 064056 (2021).
- Akdemir, K. Z., Kern, J. D. & Lamontagne, J. Assessing risks for New England's wholesale electricity market from wind power losses during extreme winter storms. *Energy* **251**, 123886 (2022).
- Busby, J. W. et al. Cascading risks: Understanding the 2021 winter blackout in Texas. *Energy Res. Soc. Sci.* **77**, 102106 (2021).
- CAISO. *Final Root Cause Analysis: Mid-August 2020 Extreme Heat Wave Tech*. <http://www.caiso.com/Documents/Final-Root-Cause-Analysis-Mid-August-2020-Extreme-Heat-Wave.pdf> (2020).
- Cao, X., Dai, X. & Liu, J. Building energy-consumption status worldwide and the state-of-the-art technologies for zero-energy buildings during the past decade. *Energy Build.* **128**, 198–213 (2016).
- Steinberg, D. et al. *Electrification and Decarbonization: Exploring U.S. Energy Use and Greenhouse Gas Emissions in Scenarios with Widespread Electrification and Power Sector Decarbonization* (National Renewable Energy Lab. (NREL), 2017).
- Waite, M. & Modi, V. Electricity load implications of space heating decarbonization pathways *Joule* **4**, 376–394 (2020).
- Mai, T. T. et al. *Electrification Futures Study: Scenarios of Electric Technology Adoption and Power Consumption for the United States* (National Renewable Energy Lab. (NREL), 2022).
- Lee, J.-Y. et al. en. in *Future Global Climate: Scenario-based Projections and Near-term Information* (eds Masson-Delmotte, V. et al.) 1–195 (IPCC, 2021).
- Seneviratne, S. I., Donat, M. G., Mueller, B. & Alexander, L. V. No pause in the increase of hot temperature extremes. *Nat. Clim. Change* **4**, 161–163 (2014).
- Sailor, D. J. Risks of summertime extreme thermal conditions in buildings as a result of climate change and exacerbation of urban heat islands. *Build. Environ.* **78**, 81–88 (2014).
- Shukla, P. R. et al. *Climate Change and Land: An IPCC Special Report on Climate Change, Desertification, Land Degradation, Sustainable Land Management, Food Security, and Greenhouse Gas Fluxes in Terrestrial Ecosystems* (IPCC, 2019).
- Cohen, J. et al. Recent Arctic amplification and extreme mid latitude weather. *Nat. Geosci.* **7**, 627–637 (2014).
- Barnes, E. A. Revisiting the evidence linking Arctic amplification to extreme weather in midlatitudes. *Geophys. Res. Lett.* <https://doi.org/10.1002/grl.50880> (2013)
- Hersbach, H. et al. The ERA5 global reanalysis. *Q. J. R. Meteorol. Soc.* **146**, 1999–2049 (2020).
- Kirschen, D. S. & Strbac, G. *Fundamentals of Power System Economics* (John Wiley & Sons, Sept. 2018).
- ERCOT. *2022 ERCOT System Planning: Long-Term Hourly Peak Demand and Energy Forecast*. https://www.ercot.com/files/docs/2022/02/24/2022_LTLF_Report.pdf (2022).
- Mathy, S., Criqui, P., Knoop, K., Fishedick, M. & Samadi, S. Uncertainty management and the dynamic adjustment of deep decarbonization pathways. *Clim. Policy* **16**, S47–S62 (2016).
- Pachauri, R. K. et al. *Climate Change 2014: Synthesis Report. Contribution of Working Groups I, II and III to the Fifth Assessment Report of the Intergovernmental Panel on Climate Change* (eds Pachauri, R. K. & Meyer, L.) 151 (IPCC, 2014).
- Jiang, A., Zhu, Y., Elsafty, A. & Tumeo, M. Effects of global climate change on building energy consumption and its implications in Florida. *Int. J. Constr. Educ. Res.* <https://doi.org/10.1080/15578771.2017.1280104> (2018).
- Rangwala, I. & Miller, J. R. Climate change in mountains: a review of elevation-dependent warming and its possible causes. *Clim. Change* **114**, 527–547 (2012).
- Ma, C., Fassnacht, S. & Kampf, S. How temperature sensor change affects warming trends and modeling: an evaluation across the State of Colorado. *Water Resour. Res.* **55**, 9748–9764 (2019).
- CIESIN. *Gridded Population of the World, Version 4 (GPWv4)* (Socioeconomic Data and Applications Center (SEDAC), 2016).
- Pudjianto, D. et al. Smart control for minimizing distribution network reinforcement cost due to electrification. *Energy Policy* **52**, 76–84 (2013).
- Watkins, G. P. A Third factor in the variation of productivity: the load factor. *Am. Econ. Rev.* **5**, 753–786 (1915).
- Nelson, T. & Orton, F. Australia's National Electricity Market: optimising policy to facilitate demand-side response. *Aust. Econ. Rev.* **49**, 146–168, <https://onlinelibrary.wiley.com/doi/abs/10.1111/1467-8462.12151> (2022).
- Poulin, A., Dostie, M., Fournier, M. & Sansregret, S. Load duration curve: A tool for technico-economic analysis of energy solutions. *Energy Build.* **40**, 29–35 (2008).
- Waite, M. et al. Global trends in urban electricity demands for cooling and heating. *Energy* **127**, 786–802 (2017).
- EPA. *Emissions & Generation Resource Integrated Database (eGRID)*. <https://www.epa.gov/egrid> (2022).
- Coles, S. *An Introduction to Statistical Modeling of Extreme Values*. <http://link.springer.com/10.1007/978-1-4471-3675-0> (2022).
- Alipour, P., Mukherjee, S. & Nateghi, R. Assessing climate sensitivity of peak electricity load for resilient power systems planning and operation: a study applied to the Texas region. *Energy* **185**, 1143–1153 (2019).
- Shaffer, B., Quintero, D. & Rhodes, J. Changing sensitivity to cold weather in Texas power demand. *iScience* **25**, 104173 (2022).
- Lee, J. & Dessler, A. E. The impact of neglecting climate change and variability on ERCOT's forecasts of electricity demand in Texas. *Weather Clim. Soc.* <https://doi.org/10.1175/WCAS-D-21-0140.1> (2022).
- Helsel, D. R. & Hirsch, R. M. *Statistical Methods in Water Resources* (Elsevier, 1992).
- Pohlert, T. *trend: Non-Parametric Trend Tests and Change-Point Detection*. <https://CRAN.R-project.org/package=trend> (2017).
- Livezey, R. E. & Chen, W. Y. *Statistical Field Significance and Its Determination by Monte Carlo Techniques*. *Monthly Weather Rev.* <https://doi.org/10.1175/1520-0493> (1983).
- Krishnamurthy, C. K. B., Lall, U. & Kwon, H.-H. Changing frequency and intensity of rainfall extremes over India from 1951 to 2003. *J. Clim.* <https://doi.org/10.1175/2009JCLI2896.1> (2009).

Acknowledgements

The work described in this paper was partially supported by InnoHK initiative, The Government of the HKSAR, and Laboratory for AI-Powered Financial Technologies. Y.A. acknowledges support from the Cheung-Kong Innovation Doctoral Fellowship. We acknowledge Dr. Ed Rubin and two anonymous reviewers for their helpful reviews which improved the manuscript.

Author contributions

Y.A. developed the code and performed the computations while U.L. conceived the idea for the study. Y.A., D.J.F. and J.D.-G. designed the analysis and conceived experiments with supervision from U.L. and V.M. All authors discussed and contributed to the final manuscript.

Competing interests

The authors declare no competing interests.

Additional information


Supplementary information The online version contains supplementary material available at <https://doi.org/10.1038/s43247-023-01048-1>.

Correspondence and requests for materials should be addressed to Yash Amonkar.

Peer review information *Communications Earth & Environment* thanks Edward Rubin and the other, anonymous, reviewer(s) for their contribution to the peer review of this work. Primary Handling Editors: Alessandro Rubino, Clare Davis. A peer review file is available.

Reprints and permission information is available at <http://www.nature.com/reprints>

Publisher's note Springer Nature remains neutral with regard to jurisdictional claims in published maps and institutional affiliations.

 **Open Access** This article is licensed under a Creative Commons Attribution 4.0 International License, which permits use, sharing, adaptation, distribution and reproduction in any medium or format, as long as you give appropriate credit to the original author(s) and the source, provide a link to the Creative Commons licence, and indicate if changes were made. The images or other third party material in this article are included in the article's Creative Commons licence, unless indicated otherwise in a credit line to the material. If material is not included in the article's Creative Commons licence and your intended use is not permitted by statutory regulation or exceeds the permitted use, you will need to obtain permission directly from the copyright holder. To view a copy of this licence, visit <http://creativecommons.org/licenses/by/4.0/>.

© The Author(s) 2023